mathematics

Article

Light Pollution Index System Model Based on Markov Random Field

Liangkun Fang [1], Zhangjie Wu [2], Yuan Tao [3] and Jinfeng Gao [2,*]

1 School of Science, Zhejiang Sci-Tech University, Hangzhou 310018, China
2 School of Information Science and Engineering, Zhejiang Sci-Tech University, Hangzhou 310018, China
3 School of Economics and Management, Zhejiang Sci-Tech University, Hangzhou 310018, China
* Correspondence: jfgao@zstu.edu.cn

Abstract: Light pollution is one of the environmental pollution problems facing the world. The research on the measurement standard of light pollution is not perfect at present. In this paper, we proposed a Markov random field model to determine the light pollution risk level of a site. Firstly, the specific data of 12 indicators of 5 typical cities were collected, and 10-factor indicators were screened using the R-type clustering algorithm. Then, the entropy weight method was used to determine the weight, and the light pollution measurement method of the Markov random field was established. The model was tested by five different data sets, and the test results show that the model is very effective. Three kinds of potential effects were proposed, and the relationship between the factor index and potential effects was established by using the partial least square method. Three possible intervention strategies for solving the problem of light pollution are pointed out: road lighting system planning, increasing vegetation coverage, and building system planning. Finally, a simulated annealing algorithm was used to determine the best intervention strategy, concluding that using strategy 1 in urban neighborhood 2 was the most effective measure, reducing the risk level of light pollution by 17.2%.

Keywords: light pollution; entropy weight method; Markov random fields; simulated annealing algorithm

MSC: 60G60

Citation: Fang, L.; Wu, Z.; Tao, Y.; Gao, J. Light Pollution Index System Model Based on Markov Random Field. *Mathematics* **2023**, *11*, 3030. https://doi.org/10.3390/math11133030

Academic Editor: Andrea Scozzari

Received: 15 June 2023
Revised: 30 June 2023
Accepted: 3 July 2023
Published: 7 July 2023

1. Introduction

Recently, with the increasing improvement in material life and cultural demands, people pay increasing attention to the pursuit of a favorable light environment. Light pollution has generated huge costs, reaching nearly USD 7 billion annually in the United States [1]. According to Gaston et al. [2], over one-tenth of the land area on Earth is illuminated by artificial light at night. Furthermore, if skylight is included, this proportion will increase to 23%. To assess the risk level of light pollution in the economic system, it is necessary to establish a widely applicable measurement standard. However, nowadays, the overall causal system of light pollution remains incomplete. There are gaps in the evaluation system and pollution mechanisms of light pollution.

Light pollution refers to unnecessary, inappropriate, or excessive artificial lighting [1]. Regarding the composition of light pollution, light pollution is generally divided into white light pollution, daytime pollution, and color pollution. With the attention paid to the problem of light pollution, an increasing number of scholars have conducted research on the causes of light pollution. The cause of light pollution is not only attributed to one factor but is the result of a complex interaction of many factors, including transportation [3], mineral resources [3], topography [3], and income [4,5]. All of these contribute to varying degrees of light pollution. Sung et al. [6] believed that light pollution is affected by residential density at the same height. The above are all studies on the causes of light pollution. At the same time, many scholars have studied the effects of light pollution. When the concept of light pollution was first introduced, governments and scholars focused on its impact on astronomical phenomena [7]. According to the study by National Geographic, the main effect of light pollution can be divided into three aspects, thus determining the risk level of light pollution in the economic system, social system, and ecosystem, respectively.

Despite some robust strategies adopted by community officials and local groups to try to slow down or eliminate light pollution, the fact remains that light pollution levels are gradually increasing. Its influence is growing. It is supposed that the effects of light pollution are mainly divided into negative effects and positive effects. The negative effects are mainly on animals [8–10] and human health [11–13]. Owens et al. [8] explored that artificial light at night would affect the movement, foraging, reproduction, and predation of insects, leading to a decline in the number and total number of local insect species. McLaren et al. [9] discovered that light significantly impacted the choice of stopover sites for migratory birds. Poor-quality stopovers can be detrimental to the conservation of migratory bird species. Thiel et al. [10] calculated and analyzed that a certain degree of light pollution would interrupt the photosynthesis of plants. The effects of light pollution on human health are also multifaceted, such as sleep quality [13] and the incidence of breast cancer [11]. Cao et al. [13] obtained that light pollution would directly interfere with the natural light–dark cycle and destroy the inherent circadian rhythm of organisms, thus seriously affecting the quality of sleep. Walker et al. [11] found a significant association between ALAN and cancer. The positive effects were mainly concentrated on the decrease in crime rate [14]. However, there is considerable controversy in the academic circle on this point [15]. Steinbach et al. [15] thought that light pollution has no positive effect on road accidents or crime in England and Wales.

Chalkias et al. [16] introduced a light pollution modeling method using geographic information systems (GIS) and remote sensing (RS) techniques in an attempt to address environmental assessment problems in sensitive suburbs. When establishing light pollution indicators, Rabaza et al. [17] established a light pollution measurement model based on astronomical methods.

Garstang [18] created a map model to observe the changes in skylight at different heights and azimuths from different observation points, effectively quantifying the brightness of artificial light. Gaston et al. [19] proposed species link schemes such as limiting the duration of lighting, changing the intensity of lighting, and changing the spectral composition of lighting to reduce the harm of sunlight and light pollution. Much literature has carried out relevant studies on light pollution, but has not been able to develop a broadly applicable metric to identify the light pollution risk level of a location. This problem is very important for the study of light pollution in practice. Driven by these factors, this paper designed a light pollution measurement method to solve these problems. This paper is motivated by these factors to design a consensus algorithm to solve the problems.

The main contributions of this work can be summarized as follows:

1. During the establishment of the Markov random field model, the weights obtained by the entropy weight method were multiplied by variables in the activation function, and the importance of different variables was reflected in the model so that the established model can more scientifically and accurately assess the severity of light pollution.
2. The established optimization model provides a scientific theory basis for selecting the best intervention strategy for the determined location.
3. After building the model, we conducted a comprehensive experiment on five data sets to check the validity of our model, and the test results show that the model is very effective.

The work consists of three parts. In Section 2, a Markov random field model is established to determine the light pollution risk level of a site, and a comprehensive experiment is conducted on five data sets to verify the validity of the model. Section 3 proposes the potential impact and intervention strategies, and the relationship between the potential impact and indicators is established. In Section 4, an optimization model for selecting the best intervention strategy is established, and the optimal intervention strategy results are obtained by testing the selected sites.

2. Development of a Broadly Applicable Metric

A broadly applicable metric was developed to determine the level of light pollution risk at a specific site. First, the main influencing factors of light pollution, namely indicators, were selected. Then, the data of corresponding indicators in different locations were collected and used to determine the evaluation system of light pollution.

2.1. Index Determination and Data Collection

Xiang et al. [3] used calibrated night-time light images to study spatial–temporal changes in light pollution in China's PAs from 1992 to 2012 and found that the impact of light pollution can be influenced by various factors, such as the local level of development, population, biodiversity, and geography. To better understand the complex relationship between these factors and the extent of light pollution, it is crucial to establish a comprehensive set of indicators. These factors have been identified, analyzed, and distilled into 12 indicators, which have been used to develop a location-based light pollution risk assessment index (LBLPRAI). The index is designed to provide a standardized way to assess the level of light pollution risk across different locations.

The LBLPRAI is a valuable tool for policymakers and stakeholders to evaluate the severity of light pollution in specific locations and to prioritize appropriate mitigation measures. As shown in Figure 1, the 12 indicators include disposable income per capita, floor area of the building, number of cars per capita, the proportion of urban population, electricity consumption per capita, night light intensity, density of population, amount of precipitation, medial humidity, average temperature, vegetation coverage, and number of species. These indicators have been carefully selected to represent the different aspects of light pollution and capture each location's unique characteristic to demonstrate the effectiveness of LBLPRAI, and specific data have been collected for 12 indicators 5 five typical Chinese cities, as reported in the 2022 China Statistical Yearbook and the 2022 China Sleep Research Report. By examining the data for each indicator, a better understanding of the relationship between the extent of light pollution and the various factors that contribute to it in different locations can be gained.

2.2. The Establishment of LBLPRAI

In the process of system analysis or evaluation, to avoid missing some important factors, as many indicators as possible are considered when selecting indicators at the beginning. However, the number of variables is too large, and the degree of correlation between variables is too high, which brings great inconvenience to analysis and modeling. Indicator data were collected from 5 representative cities, and, in order to determine the distance between clusters, Euclidean distance was used and an R-type clustering algorithm was chosen to perform clustering analysis on 12 variables [20,21]. The results are shown in Figure 2.

It can be seen from Figure 2 that per capita disposable income is grouped with the number of cars per capita, and the average humidity is grouped with moderate temperature. The factor index after clustering is ten items. Through correlation analysis [22] between different indicators, these two categories have a high degree of correlation, as shown in Figure 3.

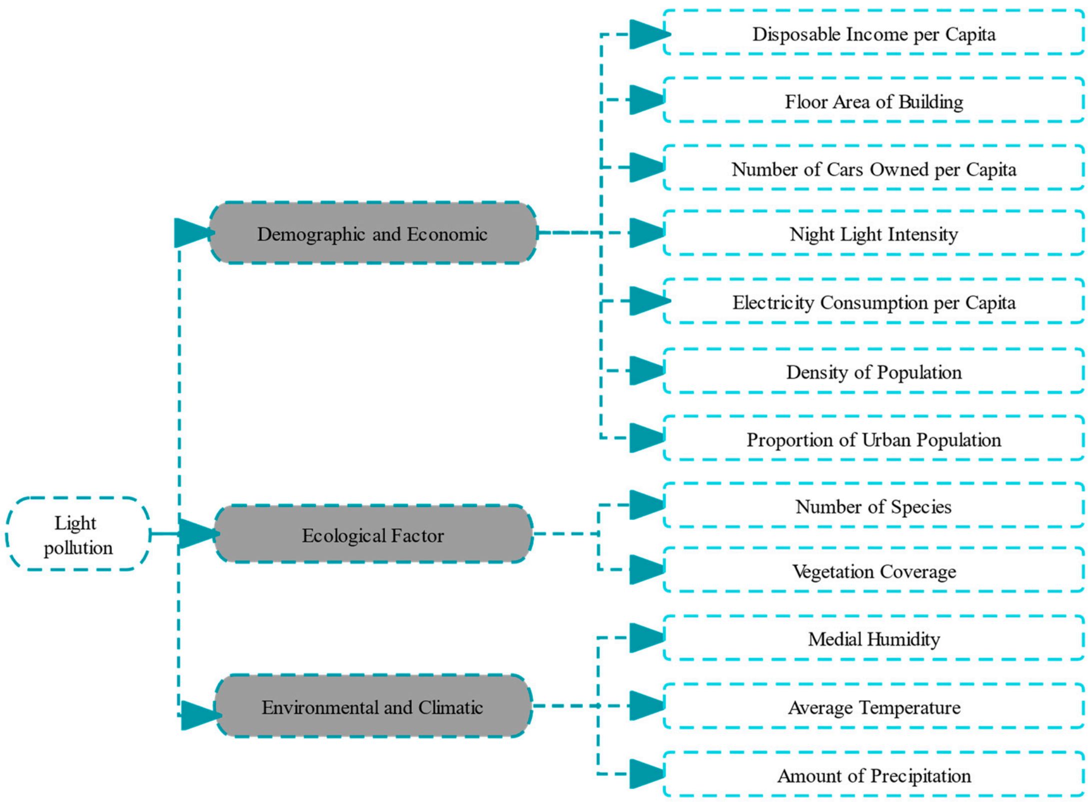

Figure 1. Location-based light pollution risk assessment index.

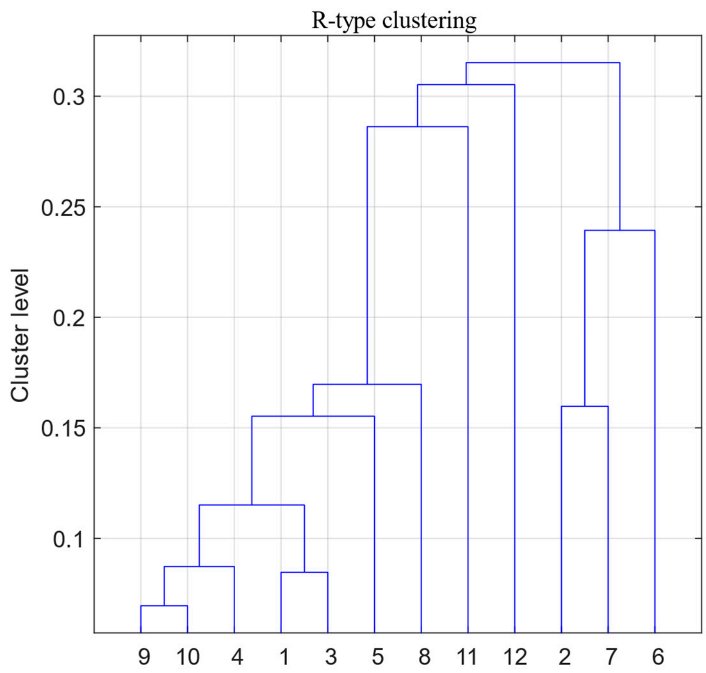

1.Disposable income per capita
2.Floor area of the building
3.Number of cars per capita
4.Proportion of urban population
5.Electricity consumption per capita
6.Night light intensity
7.Density of population
8.Amount of precipitation
9.Medial humidity
10.Average temperature
11.Vegetation coverage
12.Number of species

Figure 2. The result of the R-type cluster.

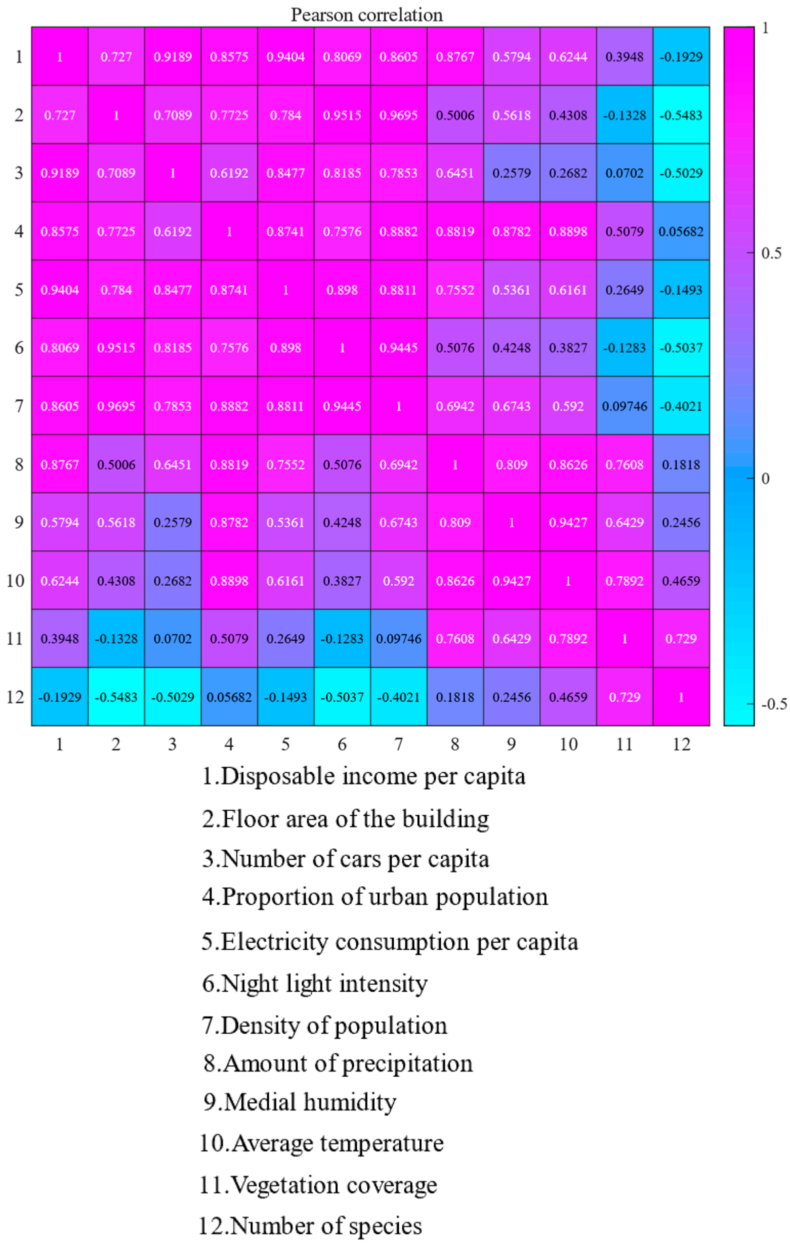

Figure 3. Correlation analysis.

The correlation coefficient between per capita disposable income and the number of cars per capita was 0.92, and the correlation coefficient between the average humidity and average temperature was 0.94. The correlation coefficients of these two categories are high, so the above four indicators were clustered into two.

According to the variation degree of each index, information entropy was used to calculate the entropy weight of each index to obtain a relatively objective index weight. Before this, partial negative data need to be processed to make all indicators positively correlated with light pollution. T_i indicates raw data, and t_i indicates processed data.

$$t_i = 2\max_i(T_i) - T_i, \tag{1}$$

After standardizing the data, the entropy weight method was established [23,24] to analyze the weight. There are $n = 5$ evaluation objects and $m = 10$ indicator variables, and the value of the ith evaluation object regarding the jth indicator variable is a_{ij} for

$i = 1, 2, \ldots, n, j = 1, 2, \ldots, m$. The data matrix $A = (a_{ij})_{n \times m}$ was constructed. The proportion of the ith evaluation object with respect to the jth index variable was calculated:

$$p_{ij} = \frac{a_{ij}}{\sum_{i=1}^{n} a_{ij}}, \ i = 1, 2, \ldots, n, \ j = 1, 2, \ldots, m. \tag{2}$$

The entropy value and coefficient of variation of the jth index variable was calculated:

$$e_j = -\frac{1}{lnn} \sum_{i=1}^{n} p_{ij} ln p_{ij}, \ g_j = 1 - e_j, \ j = 1, 2, \ldots, m. \tag{3}$$

Thus, the weight of the jth index variable was obtained:

$$k_j = \frac{g_j}{\sum_{j=1}^{m} g_j}, \ j = 1, 2, \ldots, m. \tag{4}$$

According to the data collected above, the weight of each indicator obtained is shown in Figure 4. It is found that the weight of the building area and highway lighting brightness is the largest, reaching 0.24 and 0.35, respectively, indicating that these two indexes have a more significant impact on the dedication level of light pollution.

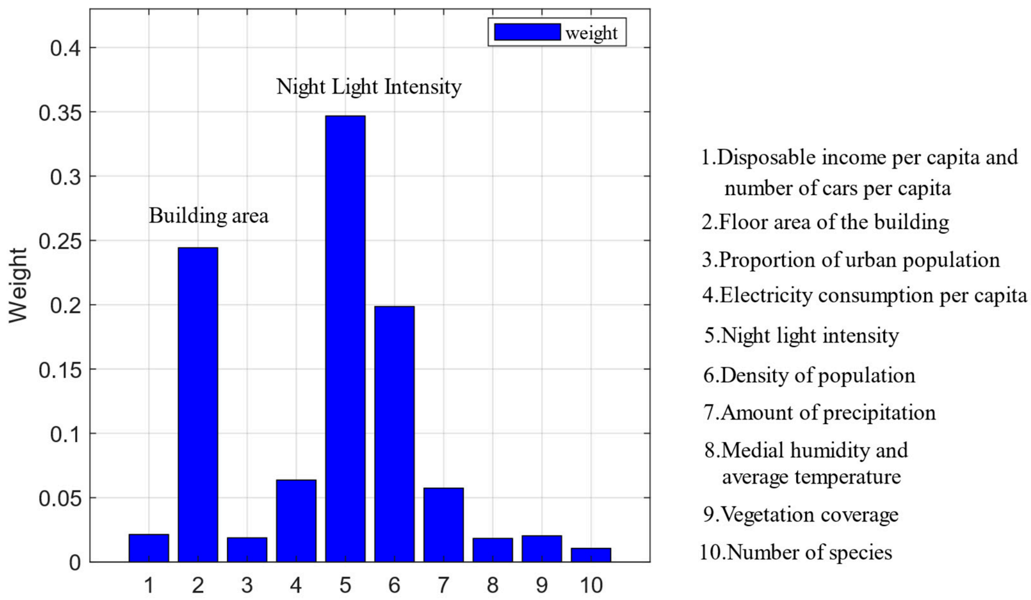

Figure 4. The weight of the index.

To develop a broadly applicable metric for measuring the level of light pollution risk, the clustering results and the indicator classes were first used, to which different indicators belong. The ten indicators were classified into three impact indicators: demographic and economic factors, environmental and climatic factors, and ecological factors, denoted as E, F, and T, respectively. It is believed that average light intensity can represent the risk level of light pollution, and all three indexes can affect the risk level of light pollution. The relationship between these indicators can be represented by the undirected probability graph, as shown in Figure 5. The boxes indicate indicators, and the lines indicate that they are correlated but not wholly causal. The posterior probability of risk index was modeled as an exponential family distribution, which can better deal with the complex relationship between different indicators. By modeling these indicators as Markov random fields [25,26], their interactions can be better understood and provide more scientific methods and tools for risk assessment and control.

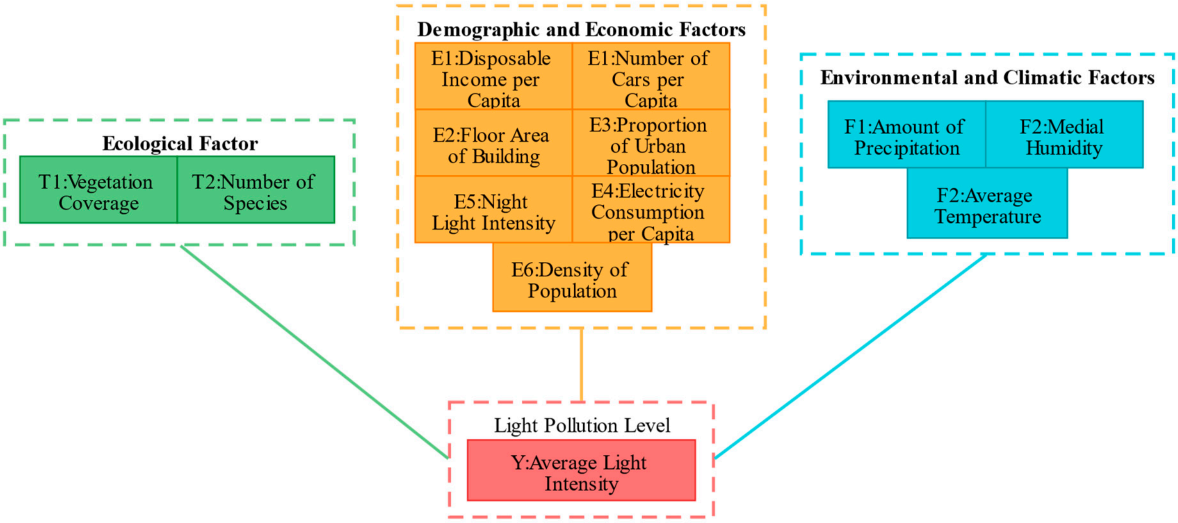

Figure 5. Undirected probability graph.

Conditional probability can be decomposed into the product of multiple exponential distributions as follows:

$$P(W|E,F,T) = \frac{1}{K}\varphi_E(E,W) * \varphi_F(F,W) * \varphi_T(T,W), \tag{5}$$

where W represents the random variable average light intensity, φ represents the exponential distribution, and K is a constant so that the value range of the right formula is $[0,1]$.

$$\varphi_E(E,W) = e^{\Lambda_1(\frac{E}{W})}. \tag{6}$$

Considering the different weights of different indicators in the index class E, the indicators were multiplied with the corresponding weights and the activation function [27] σ was increased.

$$\varphi_E(E,W) = e^{\sigma(\Lambda_1(\frac{Ek}{W}))}, Ek = \left(E_j \times k_j\right)_{m_1 \times 1}, \tag{7}$$

Thus, (5) is equal to

$$P(W|E,F,T) = \frac{1}{K}e^{\sigma(\Lambda_1(\frac{Ek}{W}))} * e^{\sigma(\Lambda_2(\frac{Fk}{W}))} * e^{\sigma(\Lambda_3(\frac{Tk}{W}))}, \tag{8}$$

where the activation function is

$$\sigma = \frac{1}{1+e^{-x}}. \tag{9}$$

Next, the Λ in the above formula was determined by using the maximum likelihood method.

$$\begin{aligned} L(\lambda) &= \log\left(\prod_{i=1}^{n} P\left(W^i|E^i,F^i,T^i\right)\right) \\ &= \sum_{i=1}^{n}\left[\sigma(\Lambda_1\left(\frac{E^ik}{W^i}\right)) + \sigma(\Lambda_2\left(\frac{F^ik}{W^i}\right)) + \sigma(\Lambda_3\left(\frac{T^ik}{W^i}\right))\right]. \end{aligned} \tag{10}$$

Using the collected data and taking the minimum loss function as the objective, the parameter Λ can be obtained:

$$\hat{\Lambda} = \text{argmin } L(\lambda), \tag{11}$$

The parameters were determined for $\Lambda = (0.462, 8.079, 3.608, 0.971, 5.517, 0.770, 6.801, 2.052, 83.462, 0.655, 0.042, 6.142, 0.273)$ and the $P\left(W^i \middle| E^i, F^i, T^i\right)$ was believed to be the ith LBLPRAI region.

After building the model, we needed to conduct a comprehensive experiment on five data sets to verify the validity of our model. Different locations were categorized into four types:

- Protected land: Areas that are protected by government or private entities from development for their ecological, cultural, and natural importance;
- Rural community: A community located in one of the sparsely populated areas of a country or region and is not easily accessible from urban communities;
- Suburban communities: Located in areas with moderate population density in a country or region or easily accessible from urban communities;
- Urban community: A community located in one of a country or region's most densely populated areas.

The light pollution risk levels of four different types of sites were obtained by collecting the data from four different types of locations and bringing the model established before into the accurate data calculation. The reasons for the results are analyzed below.

2.3. LBLPRAI of Four Diverse Types of Locations

The data were collected from five different areas, including one protected land, one rural, one suburban, and two urban communities. In this paper, LBLPRAI analysis was conducted on them, respectively, and the results were obtained as shown in Table 1.

Table 1. Light pollution risk level.

Region	LBLPRAI	Rank
Protected Land	0.02757	5
Rural Community	0.10872	4
Suburban Community	0.15159	3
Urban Community 1	0.29164	2
Urban Community 2	0.42049	1

LBLPRAI was used to measure the degree of light pollution. Namely, an increase in LBLPRAI corresponds to a greater severity of light pollution. According to the results in Table 1, light pollution in protected land is the least, followed by that in rural, suburban, and urban communities.

In order to visually see the influence and relationship of four different types of areas on the risk level of light pollution under the indicators selected, it was assumed that the data of an indicator are usually distributed in the same type of region. A total of 100 values were taken that fit the normal distribution, so 100 sets of 10-dimensional data were obtained in the same type of location. Equation (2) was used to calculate the LBLPRAI of each data collection and calculate its cumulative distribution probability:

$$F(x) = P(X < x). \tag{12}$$

The cumulative distribution function for different regions was plotted as shown in Figure 6.

It can be seen from Figure 6 that LBLPRAI values in urban communities are more extensive and distributed in a broader range, and LBLPRAI values in protected land are primarily distributed in the range $[0, 0.1]$. This result indicates that the selected index can distinguish the region type of the data by its influence on the LBLPRAI value.

The test results are in agreement with the practice, which shows that the model is very effective. Therefore, LBLPRAI provides a valuable analysis and evaluation that helps us to better understand the problem of light pollution and provides insights for developing more effective measures to control light pollution.

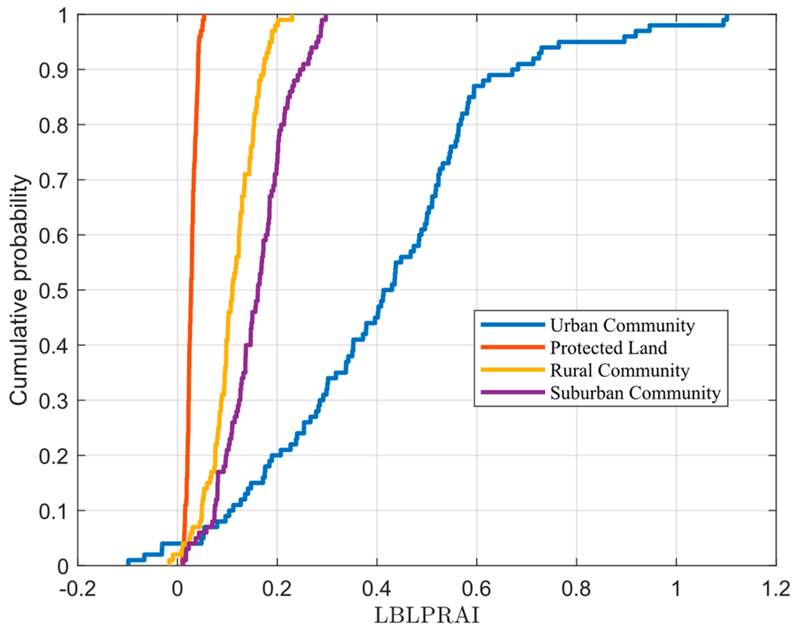

Figure 6. Cumulative distribution function.

3. Three Possible Intervention Strategies to Address Light Pollution

As shown in Figure 7, three possible intervention strategies are proposed to address light pollution. Some specific actions for each strategy are also provided, as well as the potential impact of these actions on the overall light pollution level. Furthermore, the relationship between potential impacts and indicators is established. According to the possible effects of light pollution [13–15], we chose the possibility of trouble, crime rate, and sleep time per capita as potential impacts.

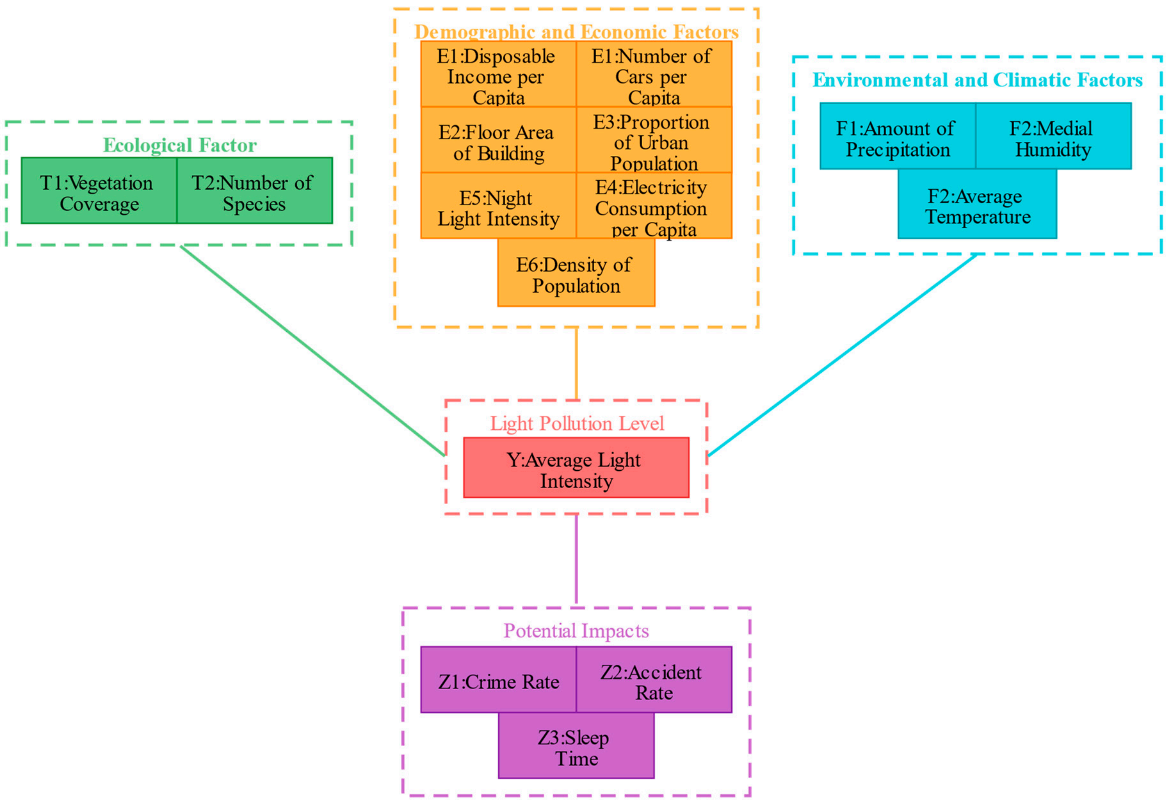

Figure 7. The relationship between potential impact and indicators.

3.1. Three Possible Intervention Strategies

Based on previous results and models, this paper proposes three broadly appropriate intervention strategies to address light pollution.

(1) Roadway lighting systems planning

This measure directly leads to the indicator "Night Light Intensity" changes. x_5 means the "Night Light Intensity" before the implementation of the intervention strategy, $\widetilde{x}_5$ represents the "Night Light Intensity" after the implementation of the intervention strategy, and μ_1 represents the implementation intensity of the intervention strategy:

$$\widetilde{x}_5 = \mu_1 x_5, \mu_1 \in [0.5, 1]. \tag{13}$$

(2) Increasing vegetation coverage

This measure directly leads to changes in the indicator "Vegetation Coverage". x_9 means the "Vegetation Coverage" before the implementation of the intervention strategy, $\widetilde{x}_9$ represents the "Vegetation Coverage" after the implementation of the intervention strategy, and μ_2 represents the implementation intensity of the intervention strategy:

$$\widetilde{\mathrm{x}}_9 = \mathrm{\mu}_2 \mathrm{x}_9, \mathrm{\mu}_2 \in [0.5, 1]. \tag{14}$$

(3) Building system planning

This measure directly leads to changes in the indicator "Floor Area of Building". x_2 means the "Vegetation Coverage" before the implementation of the intervention strategy, $\widetilde{x}_2$ represents the "Vegetation Coverage" after the implementation of the intervention strategy, and μ_3 represents the implementation intensity of the intervention strategy:

$$\widetilde{x}_2 = \mu_3 x_2, \mu_3 \in [0.5, 1]. \tag{15}$$

3.2. Potential Impacts

Firstly, potential impact indicators were selected to examine the effectiveness of the three proposed measures and explore their potential impacts. Since some communities that choose to implement low-light policies may experience an increase in crime rates, we selected the possible impact indicator of crime rate and denoted it as z_1. Similarly, reducing the use of lighting may lead to an increase in traffic accident frequency [14,15], so we selected the potential impact indicator of accident rate and denoted it as z_2. Light pollution also has an impact on wildlife and plants [13], so we selected the potential impact indicator of "Sleep Time Per Capita" and denoted it as z_3.

Different strategies will not only lead to changes in the risk level of light pollution but also affect potential indicators. The focus of partial least squares regression (RLS) research [28,29] developed in recent years is that multiple dependent variables can model multiple dependent variables regression, which can be modeled under the condition that multicollinearity exists between independent variables and has a solid ability to explain dependent variables. Partial least squares regression analysis was used to establish the relationship between different indicator variables and three potential impact indicators.

Let $x_1, x_2, \ldots, x_{10}$ represent the indicator variables and z_1, z_2, z_3 represent the potential impact indicators. We have $n = 5$ evaluation objects, $m = 10$ indicator variables, and $p = 3$ potential impact indicators. After data standardization, the data matrices $A = (a_{ij})_{n\times m}$ and $B = (a_{ij})_{n\times m}$ were constructed.

The first pair of components from two variable sets were extracted while maximizing their correlation.

$$\max\theta = \rho A^T B\gamma, \quad \begin{cases} \|\rho\|^2 = 1, \\ \|\gamma\|^2 = 1. \end{cases} \tag{16}$$

Suppose that the regression model is

$$\begin{cases} A = u\sigma^T + A_1, \\ B = u\tau^T + B_1, \end{cases} \tag{17}$$

where A_1 and B_1 state in the residual error matrix that $u = A$, $\sigma = \left[\sigma_1, \sigma_2, \ldots, \sigma_p\right]^T$, $\tau = \left[\tau_1, \tau_2, \ldots, \tau_p\right]^T$ for the parameter vector in the regression model, using the least squares estimate parameter vector:

$$\begin{cases} \sigma = \frac{A^T u}{\|u\|^2}, \\ \tau = \frac{B^T u}{\|u\|^2}. \end{cases} \tag{18}$$

Let the rank of $A = \left(a_{ij}\right)_{n\times m}$ be $r < \min(n-1, m)$, with r component $u_1, u_2, \ldots, u_r$, so that

$$\begin{cases} A = u_1\sigma^{(1)T} + \cdots + u_r\sigma^{(r)T} + A_r, \\ B = u_1\tau^{(1)T} + \cdots + u_r\tau^{(r)T} + B_r. \end{cases} \tag{19}$$

$u_i = A\rho^{(i)}$ was used to obtain the partial least squares regression equation of p potential influence indexes:

$$z = Cx + b, \tag{20}$$

where $z = \left[z_1, z_2, \ldots, z_p\right]^T$, $x = [x_1, x_2, \ldots, x_m]^T$.

The collected data were used in the model to observe each independent variable in the interpretation of $z_i (i = 1, 2, \ldots, p)$, and the regression coefficients of each coefficient were plotted in Figure 8:

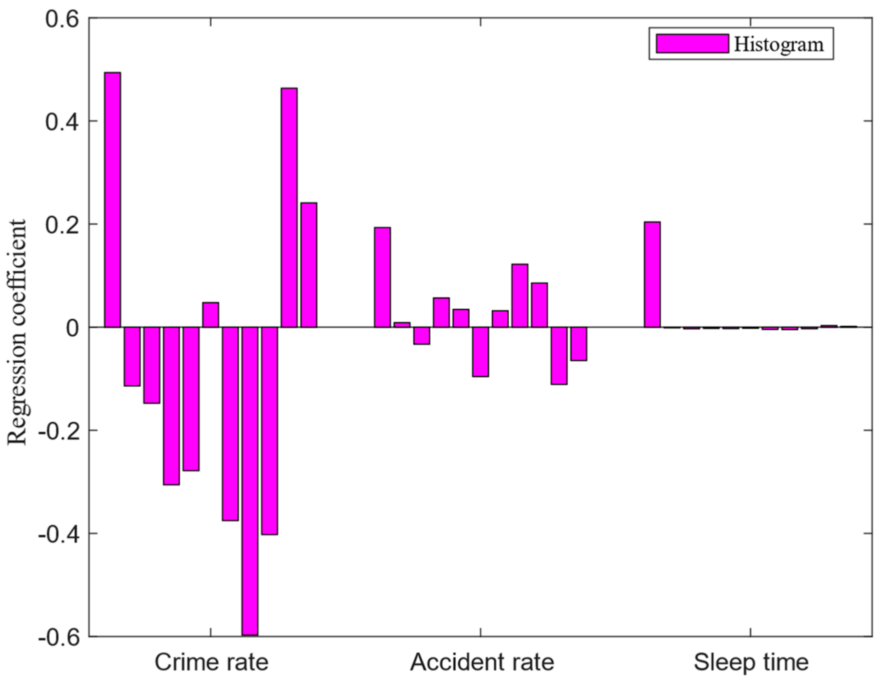

Figure 8. Regression coefficient diagram.

It can be seen from Figure 9 that disposable income per capita has a significant impact on the three potential variables, and the increase in night light intensity can reduce the crime rate to a certain extent.

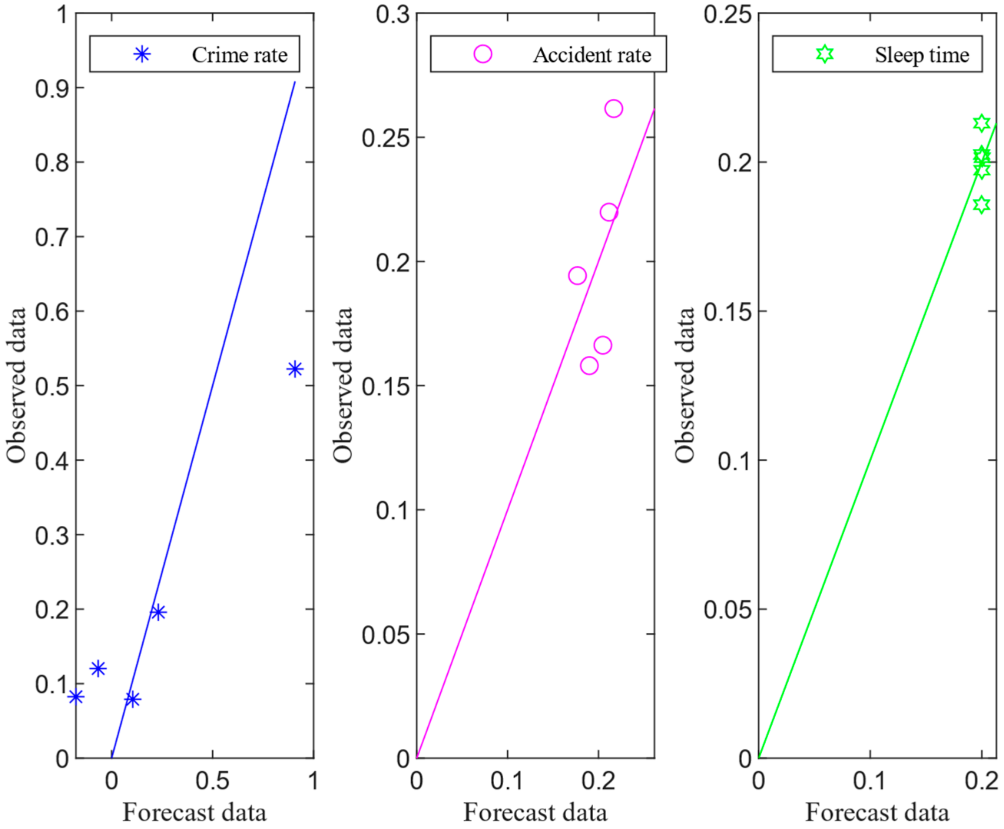

Figure 9. Sample points to draw a prediction map.

The accuracy of three regression equation models with $(\hat{z}_i, z_i)(i = 1, 2, \ldots, p)$ as the coordinate value was examined, and the prediction graph was drawn for all sample points: In this prediction chart, data points are uniformly distributed near the diagonal line, indicating that the fitting effect of the Equation is satisfactory.

3.3. Analysis and Evaluation

In order to reflect the impact of intervention strategies on the level of light pollution risk and the three potential impact indicators, the difference between the output value after adopting the intervention strategy and the true value without intervention was calculated. The change in light pollution risk level was calculated as follows:

The change in light pollution risk levels is

$$\Delta P = P\left(W^i \middle| E^i, F^i, T^i\right) - \widetilde{P}\left(W^i \middle| E^i, F^i, T^i; \mu_1, \mu_2, \mu_3\right). \tag{21}$$

The change in crime rate is

$$\Delta z_1 = z_1 - \widetilde{z}_1(\mu_1, \mu_2, \mu_3). \tag{22}$$

The change in accident rate change is

$$\Delta z_2 = z_2 - \widetilde{z}_2(\mu_1, \mu_2, \mu_3). \tag{23}$$

The change in sleep time is

$$\Delta z_3 = \widetilde{z}_3(\mu_1, \mu_2, \mu_3) - z_3. \tag{24}$$

Taking urban community 1 as an example, if strategy (1) is taken to plan the lighting intensity road lighting system and if parameter values are set as the initial value 0.5, end value 1, and step size 0.005, the light pollution risk level and the change amount of three potential influence indicators are obtained along with the curve of parameter μ_1. The results of intervention strategy (1) are shown in Figure 10.

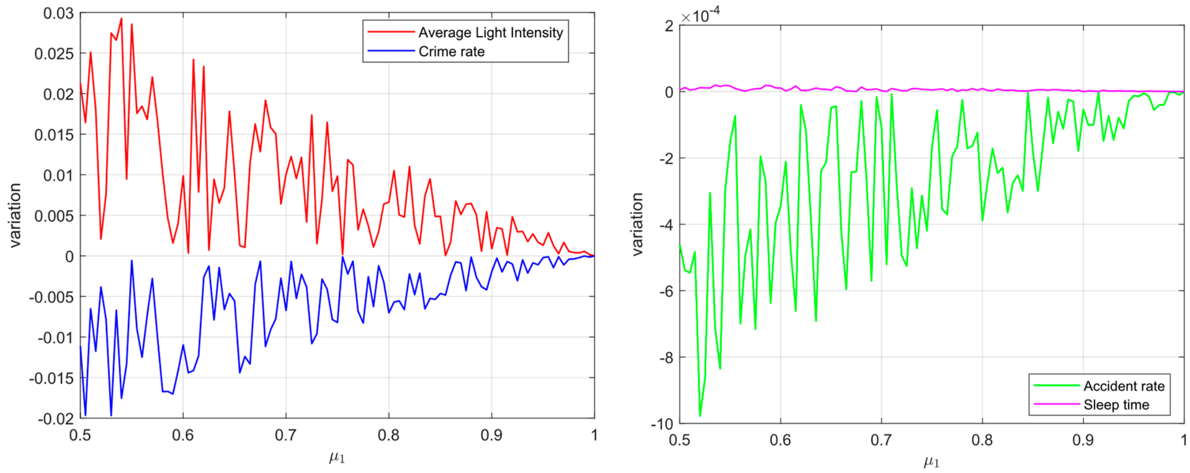

(**a**) (**b**)

Figure 10. (**a**) Intervention strategy (1) impact on light pollution level and crime rate; (**b**) intervention strategy (1) impact on accident rate and sleep time.

If intervention strategy (2) is taken to increase vegetation coverage, with the initial parameter value set to 0.5, the end value to 1, and the step size to 0.005, we can obtain the curves of the changes in light pollution risk level and the three potential impact indicators with respect to the parameter μ_2. The results of intervention strategy (2) are shown in Figure 11.

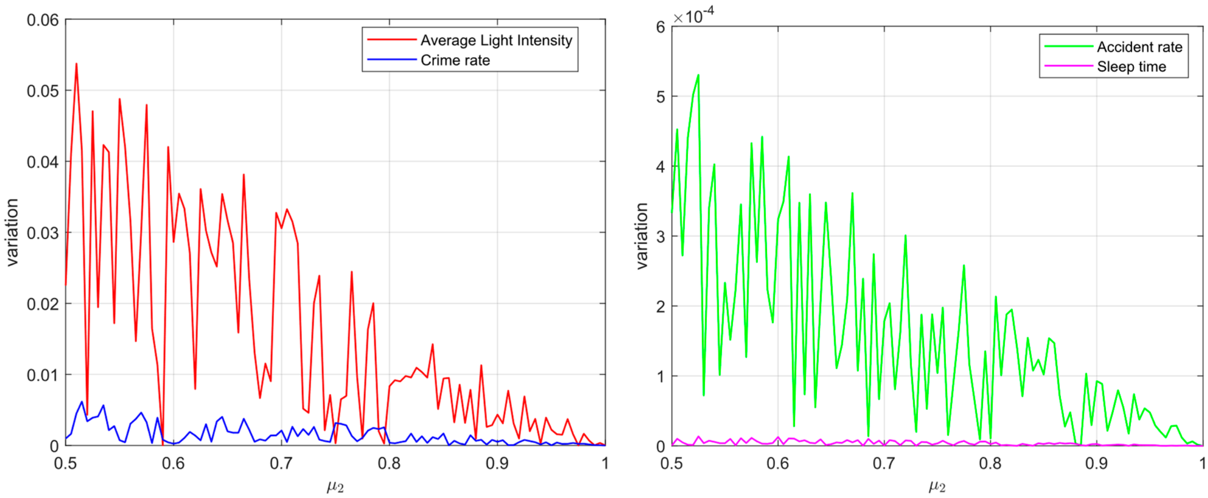

(**a**) (**b**)

Figure 11. (**a**) Intervention strategy (2) impact on light pollution level and crime rate; (**b**) intervention strategy (2) impact on accident rate and sleep time.

Taking intervention strategy (2) can lead to a significant reduction in the light pollution risk level, but its impact on the three potential impact indicators is minimal.

If intervention strategy (3) is taken, with an initial parameter value of 0.5, ending value of 1, and step size of 0.005, the change in light pollution risk level and the three potential impact indicator variables are plotted against the parameter μ_3. The results of intervention strategy (3) are shown in Figure 12.

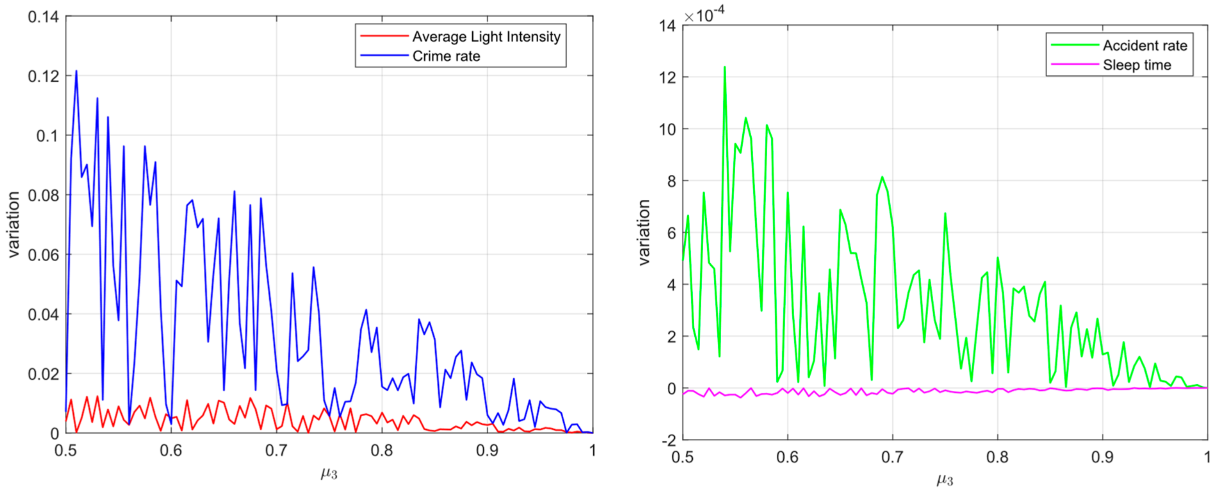

Figure 12. (**a**) Intervention strategy (3) impact on light pollution level and crime rate; (**b**) intervention strategy (3) impact on accident rate and sleep time.

Adopting intervention strategy (3) can lead to less mitigation of light pollution risk levels while also significantly reducing the crime rate and decreasing the accident rate. The impact on sleep time is not significant. Therefore, it can be seen that the reduction in building density has an important impact on the light pollution risk level and crime rate.

4. Effect of Intervention Strategies on LBLPRAI at Two Locations

In order to make the results more comparable, a site with a higher level of urbanization and a site with a lower level of urbanization should be selected for analysis. Therefore, urban community 2 and the rural community were selected as the active sites of intervention strategies, and the optimal intervention strategies were selected.

4.1. Establishment of Influence Model

In order to determine that the three intervention strategies proposed in this paper are effective in each locality, not only the impact of different intervention strategies on light pollution risk levels but also their impact on potential impact indicators need to be considered. Therefore, the optimization target was set to

$$H = \omega_1 \Delta P + \omega_2 \Delta z_1 + \omega_3 \Delta z_2 + \omega_4 \Delta z_3, \quad (25)$$

where ω_i for $i = 1, 2, 3, 4$ are weight coefficients of different influences, which are satisfied by:

$$\sum_{i=1}^{4} \omega_i = 1. \quad (26)$$

The analytic hierarchy process [30] was constructed to determine its weight coefficient, and the given judgment matrix is shown in Table 2.

Table 2. Judgment matrix.

Validity Index	ΔP	Δz_1	Δz_2	Δz_3
ΔP	1	2	2	3
Δz_1	1/2	1	1	2
Δz_2	1/2	1	1	2
Δz_3	1/3	1/2	1/2	1

The analytic hierarchy process was used to determine the weight coefficient of $\omega_1 = 0.4236$, $\omega_2 = 0.2270, \omega_3 = 0.2270, \omega_4 = 0.1223$.

Different intervention strategies will have other effects on the above indicators. To make the impact as evident as possible, an optimization model was built:

$$\begin{cases} \max H = \omega_1 \Delta P + \omega_2 \Delta z_1 + \omega_3 \Delta z_2 + \omega_4 \Delta z_3, \\ \Delta P = P(W|E,F,T) - \widetilde{P}(W|E,F,T;\mu_1,\mu_2,\mu_3), \\ \Delta z_1 = z_1 - \widetilde{z}_1(\mu_1,\mu_2,\mu_3), \\ \Delta z_2 = z_2 - \widetilde{z}_2(\mu_1,\mu_2,\mu_3), \\ \Delta z_3 = \widetilde{z}_3(\mu_1,\mu_2,\mu_3) - z_3, \\ \widetilde{x}_5 = \mu_1 x_5, \widetilde{x}_{10} = \mu_2 x_{10}, \widetilde{x}_2 = \mu_3 x_2, \mu_i \in [0.5,1], i = 1,2,3, \\ z = Cx + b, \widetilde{z}(\mu_1,\mu_2,\mu_3) = C\widetilde{x} + b, \\ \omega_1 = 0.4236, \omega_2 = \omega_3 = 0.2270, \omega_4 = 0.1223. \end{cases} \tag{27}$$

where $z = [z_1, z_2, z_3]^T, x = [x_1, x_2, \ldots, x_{10}]^T, \widetilde{z}(\mu_1,\mu_2,\mu_3) = \left[\widetilde{z}_1, \widetilde{z}_2, \widetilde{z}_3\right]^T$, $\widetilde{x} = \left[x_1, \widetilde{x}_2, \ldots, \widetilde{x}_5, \ldots, \widetilde{x}_{10}\right]^T$.

To isolate the impact of a single index, it is sufficient to set $\mu = 1$ for the remaining two terms.

4.2. Influence Model Solving

The rural community and urban community 2 were selected as the active sites of intervention strategies. Three intervention strategies were used separately for these two sites, and a simulated annealing algorithm [31,32] was used to solve Equation (27). The initial temperature $T_0 = 100$ and temperature attenuation coefficient $\rho = 0.95$ were set. The number of iterations was 3000 times, with a total of 6 times of solving. Solution result is shown in Table 3.

Table 3. Solution result.

Rural Community	μ	H	Urban Community 2	μ	H
Intervention Strategy (1)	0.53	0.02	Intervention Strategy (1)	0.82	0.25
Intervention Strategy (2)	0.66	0.03	Intervention Strategy (2)	0.54	0.04
Intervention Strategy (3)	0.89	0.01	Intervention Strategy (3)	0.74	0.11

It can be seen from the results that intervention strategy (2) is used in the rural community. Namely, increasing the vegetation coverage rate is the most effective measure. In urban community 2, intervention strategy (1) is used; that is, the planning of the illumination intensity road lighting system is the most effective measure.

Among them, the use of intervention strategy (2) in the rural community can reduce the light pollution risk level by 1.8%, crime rate by 9%, accident rate by 1.1%, and sleep time by 0.52%. In urban community 2, the intervention strategy (1) can reduce the light pollution risk by 17.2%, reduce the crime rate by 4%, increase the accident rate by 1.7%, and reduce the sleep time by 0.37%, which has little impact on sleep.

4.3. Influence Model Improvement

In the actual situation, community officials or local groups will take a variety of measures at the same time. By solving Equation (27), the difference is that, here, μ_i for $i = 1, 2, 3$ are variables solved by simulated annealing.

It can be seen from Table 4 that the results obtained by the improved model are better than those obtained by using a single intervention strategy, indicating that the use of three intervention strategies at the same time is the most effective method.

Table 4. The improved results.

Rural Community	μ	H	Urban Community 2	μ	H
Intervention Strategy (1)	0.56		Intervention Strategy (1)	0.84	
Intervention Strategy (2)	0.92	0.044	Intervention Strategy (2)	0.71	0.261
Intervention Strategy (3)	0.69		Intervention Strategy (3)	0.52	

5. Conclusions and Future Work

In this study, the authors proposed a Markov random field model as a measurement standard to determine the light pollution risk level of the site. The research results can compare and rank the light pollution levels in different regions and provide a scientific basis for the formulation of relevant policies. The work achievements are as follows:

1. When selecting indicators to assess the severity of light pollution in a specific location, 12 indicators were carefully selected. The combination of an R-type clustering algorithm and correlation analysis was used to screen the indicators, and the ten indicators finally selected can more accurately reflect the characteristics of different regions, covering all aspects of our living environment, more comprehensively assess the light pollution level in different regions, and better understand the relationship between light pollution degree and various factors causing light pollution in different regions.
2. Different sites were divided into four types for light pollution assessment. The cumulative distribution probability was used to analyze the degree of light pollution of different types of sites and interpret the results, which can intuitively see the impact and relationship of four different types of regions on the risk level of light pollution under the selected indicators.
3. The authors considered that different strategies will not only lead to changes in the risk level of light pollution but also affect potential indicators. Partial least squares regression was used to study the multicollinearity relationship between the indicator variables and the three potential impact indicators, determining that it has a strong ability to explain the dependent variables. After putting forward three possible intervention strategies for light pollution, the potential impact of each strategy on the overall impact of light pollution was evaluated using a partial least squares regression model.

In the future, we will add consideration to other factors that may affect light pollution levels and consider the scalability prospects from the algorithmic-leveled study toward real-word lighting conditions of society. In addition, Markov random field parameters can be optimized.

Author Contributions: Conceptualization, L.F. and Z.W.; data curation, Z.W.; formal analysis, L.F. and Z.W.; investigation, Z.W.; methodology, L.F. and Z.W.; resources, Z.W.; software, L.F.; validation, L.F., Z.W. and Y.T.; visualization, L.F.; writing—original draft, Z.W. and Y.T.; writing—review and editing, Z.W. and J.G. All authors have read and agreed to the published version of the manuscript.

Funding: This work is supported by National Natural Science Foundation of China under Grant (62073296).

Data Availability Statement: Not applicable.

Conflicts of Interest: The authors declare no conflict of interest.

Nomenclature

x_1	Disposable income per capita and number of cars per capita
x_2	Floor area of the building
x_3	Proportion of urban population
x_4	Electricity consumption per capita
x_5	Night light intensity
x_6	Density of population
x_7	Amount of precipitation
x_8	Medial humidity and average temperature
x_9	Vegetation coverage
x_{10}	Number of species

References

1. Gallaway, T.; Olsen, R.N.; Mitchell, D.M. The economics of global light pollution. *Ecol. Econ.* **2010**, *69*, 658–665. [CrossRef]
2. Gaston, K.J.; Duffy, J.P.; Gaston, S.; Bennie, J.; Davies, T.W. Human alteration of natural light cycles: Causes and ecological consequences. *Oecologia* **2014**, *176*, 917–931. [CrossRef]
3. Xiang, W.L.; Tan, M.H. Changes in light pollution and the causing factors in China's protected areas, 1992–2012. *Remote Sens.* **2017**, *9*, 1026. [CrossRef]
4. Rafindadi, A.A.; Muye, I.M.; Kaita, R.A. The effects of fdi and energy consumption on environmental pollution in predominantly resource-based economies of the gcc. *Sustain. Energy Technol. Assess.* **2018**, *25*, 126–137. [CrossRef]
5. Wu, B.; Wong, H. Visualization and analysis of light pollution: A case study in Hong Kong. *ISPRS Ann. Photogrametry Remote Sens. Spat. Inf. Sci.* **2012**, *1*, 171–176. [CrossRef]
6. Sung, C.Y. Examining the effects of vertical outdoor built environment characteristics on indoor light pollution. *Build. Environ.* **2022**, *210*, 108724. [CrossRef]
7. Riegel, K.W. Light pollution: Outdoor lighting is a growing threat to astronomy. *Science* **1973**, *179*, 1285–1291. [CrossRef]
8. Owens, A.C.S.; Cochard, P.; Durrant, J.; Farnworth, B.; Perkin, E.K.; Seymoure, B. Light pollution is a driver of insect declines. *Biol. Conserv.* **2020**, *241*, 108259. [CrossRef]
9. McLaren, J.D.; Buler, J.J.; Schreckengost, T.; Smolinsky, J.A.; Boone, M.; van Loon, E.E.; Dawson, D.K.; Walters, E.L. Artificial light at night confounds broad-scale habitat use by migrating birds. *Ecol. Lett.* **2018**, *21*, 356–364. [CrossRef]
10. Thiel, S.; Döhring, T.; Köfferlein, M.; Kosak, A.; Martin, P.; Seidlitz, H.K. A phytotron for plant stress research: How far can artificial lighting compare to natural sunlight? *J. Plant Physiol.* **1996**, *148*, 456–463. [CrossRef]
11. Walker, W.H.; Bumgarner, J.R.; Walton, J.C.; Liu, J.A.; Meléndez-Fernández, O.H.; Nelson, R.J.; DeVries, A.C. Light pollution and cancer. *Int. J. Mol. Sci.* **2020**, *21*, 9360. [CrossRef]
12. Clarke, R.B.; Amini, H.; James, P.; von Euler-Chelpin, M.; Jorgensen, J.T.; Mehta, A.; Cole-Hunter, T.; Westendorp, R.; Mortensen, L.H.; Loft, S.; et al. Outdoor light at night and breast cancer incidence in the danish nurse cohort. *Environ. Res.* **2021**, *194*, 110631. [CrossRef] [PubMed]
13. Cao, M.; Xu, T.; Yin, D.Q. Understanding light pollution: Recent advances on its health threats and regulations. *J. Environ. Sci.* **2023**, *127*, 589–602. [CrossRef]
14. Xu, Y.Q.; Fu, C.; Kennedy, E.; Jiang, S.H.; Owusu-Agyemang, S. The impact of street lights on spatial-temporal patterns of crime in detroit, michigan. *Cities* **2018**, *79*, 45–52. [CrossRef]
15. Steinbach, R.; Perkins, C.; Tompson, L.; Johnson, S.; Armstrong, B.; Green, J.; Grundy, C.; Wilkinson, P.; Edwards, P. The effect of reduced street lighting on road casualties and crime in england and wales: Controlled interrupted time series analysis. *J. Epidemiol. Community Health* **2015**, *69*, 1118–1124. [CrossRef]
16. Chalkias, C.; Petrakis, M.; Psiloglou, B.; Lianou, M. Modelling of light pollution in suburban areas using remotely sensed imagery and gis. *J. Environ. Manag.* **2006**, *79*, 57–63. [CrossRef]
17. Rabaza, O.; Galadi-Enriquez, D.; Estrella, A.E.; Dols, F.A. All-sky brightness monitoring of light pollution with astronomical methods. *J. Environ. Manag.* **2010**, *91*, 1278–1287. [CrossRef] [PubMed]
18. Garstang, R. Night sky brightness at observatories and sites. *Publ. Astron. Soc. Pac.* **1989**, *101*, 306. [CrossRef]
19. Gaston, K.J.; Davies, T.W.; Bennie, J.; Hopkins, J. Review: Reducing the ecological consequences of night-time light pollution: Options and developments. *J. Appl. Ecol.* **2012**, *49*, 1256–1266. [CrossRef]
20. Fraser, C.; Pylyavskyy, P. Tensor diagrams and cluster combinatorics at punctures. *Adv. Math.* **2023**, *412*, 108796. [CrossRef]
21. Zhou, S.; Xu, Z.; Liu, F. Method for determining the optimal number of clusters based on agglomerative hierarchical clustering. *IEEE Trans. Neural Netw. Learn. Syst.* **2016**, *28*, 3007–3017. [CrossRef]
22. Zhou, Y.; Zhang, Q.; Singh, V.P.; Xiao, M. General correlation analysis: A new algorithm and application. *Stoch. Environ. Res. Risk Assess.* **2015**, *29*, 665–677. [CrossRef]
23. Ye, J. Multicriteria fuzzy decision-making method using entropy weights-based correlation coefficients of interval-valued intuitionistic fuzzy sets. *Appl. Math. Model.* **2010**, *34*, 3864–3870. [CrossRef]

24. Deng, J.; Pandey, M. Optimal maximum entropy quantile function for fractional probability weighted moments and its applications in reliability analysis. *Appl. Math. Model.* **2023**, *114*, 230–251. [CrossRef]
25. Zhao, Q.H.; Li, X.L.; Li, Y.; Zhao, X.M. A fuzzy clustering image segmentation algorithm based on hidden markov random field models and voronoi tessellation. *Pattern Recognit. Lett.* **2017**, *85*, 49–55. [CrossRef]
26. Baz, J.; Díaz, I.; Montes, S.; Pérez-Fernández, R. Some results on the gaussian markov random field construction problem based on the use of invariant subgraphs. *Test* **2022**, *31*, 856–874. [CrossRef]
27. Zhang, H.; Wang, W.T.; Xiao, B. Exponential convergence for high-order recurrent neural networks with a class of general activation functions. *Appl. Math. Model.* **2011**, *35*, 123–129. [CrossRef]
28. Wang, Y.X.; Xu, Z.H. Statistical analysis for contract cheating in chinese universities. *Mathematics* **2021**, *9*, 1684. [CrossRef]
29. Su, Y.C.; Wu, C.Y.; Yang, C.H.; Li, B.S.; Moi, S.H.; Lin, Y.D. Machine learning data imputation and prediction of foraging group size in a kleptoparasitic spider. *Mathematics* **2021**, *9*, 415. [CrossRef]
30. Bekesiene, S.; Vasiliauskas, A.V.; Hoskova-Mayerova, S.; Vasiliene-Vasiliauskiene, V. Comprehensive assessment of distance learning modules by fuzzy ahp-topsis method. *Mathematics* **2021**, *9*, 409. [CrossRef]
31. Yu, C.Y.; Heidari, A.A.; Chen, H.L. A quantum-behaved simulated annealing algorithm-based moth-flame optimization method. *Appl. Math. Model.* **2020**, *87*, 1–19. [CrossRef]
32. He, F.; Ye, Q. A bearing fault diagnosis method based on wavelet packet transform and convolutional neural network optimized by simulated annealing algorithm. *Sensors* **2022**, *22*, 1410. [CrossRef] [PubMed]